nature immunology

Lymphotoxin regulates commensal responses to enable diet-induced obesity

Vaibhav Upadhyay[1], Valeriy Poroyko[2], Tae-jin Kim[1], Suzanne Devkota[3], Sherry Fu[1], Donald Liu[2], Alexei V Tumanov[1], Ekaterina P Koroleva[1], Liufu Deng[1], Cathryn Nagler,[1] Eugene B Chang[3], Hong Tang[4] & Yang-Xin Fu[1]

Microbiota are essential for weight gain in mouse models of diet-induced obesity (DIO), but the pathways that cause the microbiota to induce weight gain are unknown. We report that mice deficient in lymphotoxin, a key molecule in gut immunity, were resistant to DIO. *Ltbr*$^{-/-}$ mice had different microbial community composition compared to their heterozygous littermates, including an overgrowth of segmented filamentous bacteria (SFB). Furthermore, cecal transplantation conferred leanness to germ-free recipients. Housing *Ltbr*$^{-/-}$ mice with their obese siblings rescued weight gain in *Ltbr*$^{-/-}$ mice, demonstrating the communicability of the obese phenotype. *Ltbr*$^{-/-}$ mice lacked interleukin 23 (IL-23) and IL-22, which can regulate SFB. Mice deficient in these pathways also resisted DIO, demonstrating that intact mucosal immunity guides diet-induced changes to the microbiota to enable obesity.

Over two-thirds of adults in the United States are overweight or obese, and studies suggest that the incidence of obesity will continue to rise in coming decades[1–3]. Although early studies of twins suggested an important role for host genetics in obesity[4,5], recent evidence demonstrates that obesity is associated with a change in the intestinal microbiota[6,7]. Germ-free rodent models have revealed that the commensal microbiota contribute substantially to overall body weight, and even obesity induced by high-fat diet (HFD) is enervated in the absence of commensal bacteria[8,9]. Several studies have suggested that dietary components are the primary determinants of the composition of the microbiota[10,11], but how the microbiota responds to changes in diet and ultimately impacts DIO is unknown.

Mucosal immunity lies in a delicate balance with the microbiota; a consequence of this symbiosis is a reciprocal relationship between host and microbe that contribute to host health[12]. As a result, there has been great speculation into the role of mucosal homeostasis in host illness, especially in the case of obesity. Recently it has been argued that in the absence of inflammasome signaling pathogenic microbes penetrate the mucosa and result in the production of tumor necrosis factor (TNF), which causes non-alcoholic steatohepatitis in diets deficient for essential amino acids[13]. That study is similar to what has been argued for Toll-like receptor 5 (TLR5) in metabolic syndrome, where the absence of TLR5 results in a dysbiosis that induces weight gain[14]. However, although both of these studies and others have been informative of host-microbe dynamics in metabolic disease, it remains to be definitively demonstrated which mucosal immune pathways regulate the microbiota to induce normal weight gain after exposure to HFD in wild-type animals or humans.

Several epidemiological studies have linked polymorphisms in the *Tnf-Lta* locus to obesity and type II diabetes[15,16]. Although the role of TNF in obesity has been extensively studied, the role of lymphotoxin in this disease has been largely ignored. Lymphotoxin is essential for normal mucosal immunity[17–19]. Lymphotoxin alpha (LTα) forms a membrane-bound heterotrimer with LTβ and binds LTβ receptor (LTβR). Deficiency in either LTα or LTβR results in complete secondary lymphoid aplasia, including a lack of mesenteric lymph nodes, Peyer's patches and isolated lymphoid follicles[20]. The LTβR pathway directly regulates expression of IL-23, a heterodimeric cytokine composed of p19 and p40 subunits, and IL-23 induced by LTβR results in production of IL-22 from RORγt^{+} innate lymphocytes; *Ltbr*$^{-/-}$ mice do not express sufficient IL-23 and IL-22 to eliminate mucosal pathogens[21,22]. Thus, intact agonism of the lymphotoxin pathway is critical for normal mucosal defense.

Lta, the gene encoding LTα, is located 1.3 kilobases (kb) away from *Tnf*[16,20]. Mechanistic studies in mice have revealed that in the absence of TNF signaling, mice are less susceptible to insulin resistance provoked by DIO[23]. However, deficiency in TNF signaling only has a modest impact on adiposity in DIO, arguing that the activity of the TNF pathway alone does not explain changes in body mass. As a result, the polymorphisms linking TNF to obesity may be informative of an actual mechanistic connection between lymphotoxin and obesity. This notion is best illustrated by the fact that some polymorphisms linking TNF to obesity actually lie within coding exons of *Lta*[16]. A conclusion of the work on the 'obesity-associated microbiome' is that environmental exposure, either in the form of HFD or through colonization of obesity-inducing microbiota, may actually be critical

[1]Department of Pathology and Committee on Immunology, The University of Chicago, Chicago, Illinois, USA. [2]Department of Surgery, The University of Chicago, Chicago, Illinois, USA. [3]Department of Medicine, The University of Chicago, Chicago, Illinois, USA. [4]Key Laboratory of Infection and Immunity, Institute of Biophysics, Chinese Academy of Sciences, Beijing, China. Correspondence should be addressed to Y.-X.F. (yfu@uchicago.edu).

Received 3 February; accepted 23 July; published online 26 August 2012; doi:10.1038/ni.2403

in the pathogenesis of obesity and associated diseases[7]. The microbiota lie in a delicate homeostasis with host immunity, and given the epidemiological data linking lymphotoxin to obesity and the key role of lymphotoxin in regulating mucosal defense, we hypothesized that lymphotoxin-driven pathways regulate changes to the microbiota that promote weight gain in DIO.

RESULTS

LTβR and LTα are essential for weight gain in DIO

To address the role of the lymphotoxin pathway in DIO, we challenged wild-type and *Ltbr*$^{-/-}$ adult mice with HFD. We kept mice on normal chow diet (NCD) in our vivarium until 9 weeks of age when we either switched them to HFD or maintained them on NCD (for composition of all diets, see **Supplementary Table 1**). Although there was no difference in growth between wild-type and *Ltbr*$^{-/-}$ mice on NCD, wild-type mice on HFD gained significantly more weight than *Ltbr*$^{-/-}$ mice, which were resistant to DIO (**Fig. 1a**). There was no difference in weight after 9 weeks of dietary challenge between wild-type and *Ltbr*$^{-/-}$ mice maintained on NCD; wild-type and *Ltbr*$^{-/-}$ mice weighed 21.70 ± 0.60 g (mean ± s.e.m.) and 22.66 ± 0.56 g at the end of NCD, respectively (**Fig. 1b**). However, at the end of HFD, wild-type and *Ltbr*$^{-/-}$ groups were significantly different, weighing 29.13 ± 0.99 g and 22.87 ± 0.62 g, respectively (**Fig. 1b**). In contrast to wild-type mice, *Ltbr*$^{-/-}$ mice did not gain additional weight after prolonged HFD, suggesting a role for the lymphotoxin pathway in controlling excess weight gain induced by HFD.

At the end of the 9-week diet challenge, we investigated whether changes in weight gain corresponded with changes in adiposity. Necropsy revealed the perigonadal fat pad of wild-type mice was much larger than that of *Ltbr*$^{-/-}$ mice (**Supplementary Fig. 1**). To quantify these results, we dissected and weighed the perigonadal fat pad of wild-type and *Ltbr*$^{-/-}$ mice. Both in absolute terms and as a percentage of body weight, the perigonadal fat pad of wild-type mice had expanded much more than that of *Ltbr*$^{-/-}$ mice on HFD. This finding was in stark contrast to their relative adiposity on NCD, where wild-type and *Ltbr*$^{-/-}$ mice had similar weight at the end of diet and had similar body composition (**Fig. 1c** and **Supplementary Fig. 1**). These data demonstrate that LTβR is essential for excess weight gain and adiposity induced by HFD.

LTα forms part of a membrane-bound heterotrimer that binds to LTβR, and polymorphisms in coding exons of LTα have been linked to obesity[16]. We therefore challenged wild-type and *Lta*$^{-/-}$ mice with HFD to determine whether this ligand was essential for weight gain. Consistent with our results in *Ltbr*$^{-/-}$ mice, *Lta*$^{-/-}$ mice resisted DIO and exhibited growth on HFD that was similar to that of both wild-type and *Lta*$^{-/-}$ mice on NCD (**Fig. 1d**); these growth patterns reflected stark differences in body composition between wild-type and *Lta*$^{-/-}$ mice on HFD, with the latter being much leaner than the former (**Fig. 1e** and **Supplementary Fig. 1**). Similar to the case with *Ltbr*$^{-/-}$ mice, *Lta*$^{-/-}$ mice did not gain body weight on HFD, contextualizing the importance of the lymphotoxin pathway in DIO. *Ltb*$^{-/-}$ mice also resisted weight gain compared to wild-type mice on HFD (**Supplementary Fig. 2**). These data for *Lta*$^{-/-}$, *Ltb*$^{-/-}$ and *Ltbr*$^{-/-}$ mice demonstrate the importance of the intact, membrane-bound lymphotoxin pathway in DIO.

LTβR regulates the microbiota to induce weight gain

To better understand the mechanism by which the lymphotoxin pathway promoted weight gain in DIO, we addressed the food intake of wild-type and *Ltbr*$^{-/-}$ mice on NCD and HFD. There were no obvious changes in feeding behavior between groups on NCD or on HFD (**Fig. 2a**), suggesting that differences in weight gain were occurring despite similar consumption. Studies in axenic mice have revealed that the intestinal microbiota enable access to greater caloric intake, and as a result germ-free mice weigh substantially less than their conventionalized littermates[9]. Because the lymphotoxin signaling pathways have such a prominent role in normal mucosal defense and because feeding behavior was similar between groups, we wondered whether the lymphotoxin pathway influenced changes in the microbiota that promoted weight gain.

To address this issue, we amplified V1–V2 tags of hypervariable regions of genes encoding16S rRNA from stool samples obtained from *Ltbr*$^{+/-}$ and *Ltbr*$^{-/-}$ mice on NCD and HFD and subjected the resulting PCR products to 454 pyrosequencing. We performed principle coordinate analysis (PCA) to spatially discriminate the variable region tag sequences of genes encoding 16S rRNA from *Ltbr*$^{+/-}$ and *Ltbr*$^{-/-}$ stool DNA. PCA revealed genotype- and diet-specific clustering dependent on the two largest components of variation (**Supplementary Fig. 3**). PCA1 (52.18% of variation) strongly separated NCD and HFD groups and was consistent with a HFD-induced expansion of the Firmicute phyla observed in both genotypes (**Supplementary Figs. 3** and **4**); PCA2 (17.96% of variation) separated null and heterozygous mice and demonstrated differences not explained by diet alone.

In addition to Firmicute expansion, a hallmark of the 'obese microbiome' in human stool is a loss of commensal diversity. Even though total bacterial content as addressed by bacterial DNA per gram of

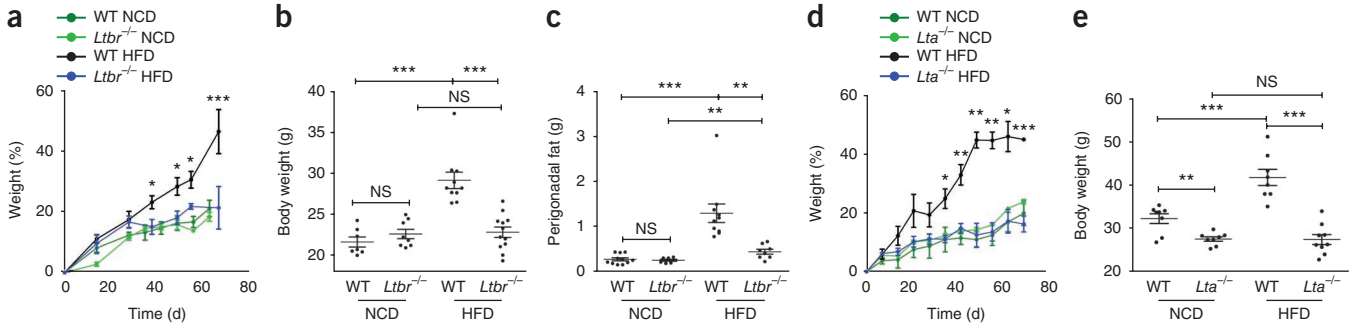

Figure 1 LTβR is essential for weight gain in response to HFD. (**a**–**e**) 9-week-old wild-type (WT; C57BL/6), *Ltbr*$^{-/-}$ or *Lta*$^{-/-}$ mice fed a HFD or NCD for 9 weeks; weight gain as a percentage of starting weight (**a**); absolute weight in grams at the end of the diet (**b**); weight of perigonadal fat at the end of diet (**c**); weight gain as a percentage of starting weight during the diet (**d**); and weight at the end of diet (**e**). Data represent 2–3 independent experiments per genotype, with $n = 5$–12 mice in all groups; statistics demonstrate differences between HFD groups; Student's *t*-test for individual points along growth curves; one-way ANOVA with Bonferroni *post-hoc* test for dot plots: $^{*}P < 0.05$, $^{**}P < 0.01$, $^{***}P < 0.001$, NS, not significant ($P > 0.05$). Error bars, s.e.m.

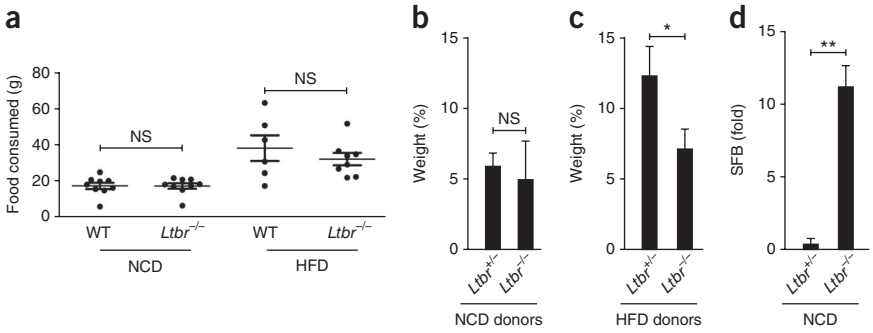

Figure 2 LTβR influences weight gain through changes in the microbiota. (**a**) Food consumed represents the weight difference of food between days *n* and *n* + 1 in a given cage of mice during the first 2 weeks on diet. (**b**,**c**) Weight gain as a percentage of starting body weight 20 d after gavage of germ-free recipients from the NCD (**b**) and HFD (**c**) donor groups with cecal contents from $Ltbr^{+/-}$ or $Ltbr^{-/-}$ littermates maintained on NCD or HFD for 9–10 weeks starting at 9 weeks of age. Cecal contents from two donors were pooled. Recipients and donor were kept on diets of similar composition. (**d**) Real-time PCR for SFB plasmid CTL5-6 on DNA from stool collected from $Ltbr^{+/-}$ and $Ltbr^{-/-}$ mice 4 weeks after the start of NCD (for **a**,**d**, $n = 4$ mice per group, representative of three experiments, Student's *t*-test; for **b**,**c**, $n = 3$–5 germ free mice per group, representative of two experiments, paired *t*-test; $^{*}P < 0.05$, $^{**}P < 0.001$), NS, not significant ($P > 0.05$). Error bars, s.e.m.

stool was similar between either genotype and diet, $Ltbr^{+/-}$ mice experienced reduced commensal diversity after the start of HFD, whereas $Ltbr^{-/-}$ mice maintained a similarly diverse community to that of either group at the start of diet (**Supplementary Fig. 4**).

Although there were no differences at the phyla level between genotypes, we observed an overgrowth of the Erysopelotrichi class after HFD in $Ltbr^{+/-}$ (obese) mice that was completely absent in $Ltbr^{-/-}$ (lean) mice after HFD (**Supplementary Table 2**); this underrepresentation of Erysopelotrichi may have occurred due to the overabundance of the Cytophagia class of the Bacteroidetes phyla (**Supplementary Table 2**). The relative abundance of both of these classes was similar between genotypes on NCD (data not shown). This is an important finding given that the Erysipelotrichi class has previously been reported as overabundant in the obese state[24], and its ability to overgrow and monopolize the gastrointestinal niche after HFD has implicated it as a species that may influence metabolic disease in the host and whose colonization status after HFD appears to depend on the LTβR.

To test how the changes to the microbiota contributed to weight gain, we transplanted the cecal contents of $Ltbr^{+/-}$ and $Ltbr^{-/-}$ mice into wild-type germ-free recipients. We maintained the recipients on a diet of similar composition to that of their donors (**Supplementary Table 1**). Consistent with our results in SPF mice, there was no difference in weight gain between recipients that received cecal contents from $Ltbr^{+/-}$ or $Ltbr^{-/-}$ donors on NCD after 20 d of diet (**Fig. 2b**), suggesting that although there were detectable differences in the microbial communities at this point, these differences seen on NCD could not explain different weight gain between genotypes. In contrast, the cecal contents of $Ltbr^{+/-}$ mice conferred greater weight gain than that of $Ltbr^{-/-}$ mice when we kept both donor and recipient groups on HFD (**Fig. 2c**). Although recipient groups had different weights 20 d after transplant and before this time, the recipients of $Ltbr^{-/-}$ cecal contents caught up in weight gain after this time point (data not shown); however, these data could be due to the fact that recipient mice are wild type and thus have an intact mucosal immune response. In wild-type gnotobiotic mice microbial communities may normalize after 3 weeks of HFD, a time period for maturation of isolated lymphoid follicles and other key elements of mucosal immunity. These data demonstrate that changes in the microbial communities colonizing $Ltbr^{+/-}$ and $Ltbr^{-/-}$ mice after HFD at least transiently caused excess weight gain in the heterozygous group after HFD.

The fecal stream is composed of allochthonous (transient) and autochthonous (permanent resident) microbes and is informative of microbiota living throughout the gastrointestinal tract[25]. Additional analysis of stool revealed changes in specific operational taxonomic units (OTUs) between heterozygous and knockout mice after 4 weeks of HFD that extended beyond the class level to that of changes in specific genera. There were several OTUs over- and underrepresented in $Ltbr^{-/-}$ mice after HFD; we focused on overrepresented species because such species appear to require an LTβR-mediated immune response for clearance from the microbiota in response to HFD. Such clearance could contribute to the loss of commensal diversity experienced by heterozygous mice after HFD was initiated (**Supplementary Fig. 4**). One OTU significantly overrepresented in $Ltbr^{-/-}$ mice was not classifiable beyond the Clostridiales order (**Supplementary Table 2**). The OTU detected in our analysis had high sequence homology with the V1-V2 region of the 16S rRNA encoding gene of SFB (**Supplementary Fig. 5**), an autochthonous, unclassified member of the Clostridiales order that can induce a potent interleukin 17–producing T helper cell (T_H17) cytokine-based immune response in mice[26–28]. SFB are detectable in the fecal stream of mice throughout adulthood but live in the mucus layer of the ileum[29,30]. Quantitative PCR with primers specific for SFB genes demonstrated that SFB experienced a moderate overgrowth in $Ltbr^{-/-}$ mice, which was detectable both in the feces and terminal ileum of mice on NCD and HFD (**Fig. 2d** and **Supplementary Fig. 6**). Therefore, the LTβR pathway regulates changes in the microbiota, including loss of commensal diversity, after the initiation of HFD.

Sibling cohousing rescued weight gain and SFB regulation

Given the conflicting viewpoints presented by various studies regarding genetic and environmental causes for obesity[4,5,7], we wondered whether environmental manipulation would influence the phenotype of LTβR-deficient mice. To explore this, we weaned $Ltbr^{+/-}$ and $Ltbr^{-/-}$ littermates into cages separated by genotype or into cages where genotypes were mixed. Mice are coprophagic, and consumption of feces is a mechanism by which mice that are housed together colonize one another with their own microbial communities; cohousing is a commonly used experimental technique to facilitate exposure of microbiota[28,31]. Separately housed $Ltbr^{-/-}$ mice resisted excess body weight induced by HFD, but $Ltbr^{-/-}$ mice housed together with their $Ltbr^{+/-}$ littermates experienced a rescued capacity for excess weight gain in response to HFD (**Fig. 3a**,**b**). These data suggest that $Ltbr^{+/-}$ littermates, which maintain intact regulation of their own microbiota, may be constantly exposing $Ltbr^{-/-}$ mice to obesity-inducing microbes and supplementing body growth. Although both $Ltbr^{+/-}$ and $Ltbr^{-/-}$ mice were exposed to the each other's microbiota, the phenotype of heterozygous mouse, which maintains an intact mucosal immune response, is dominant.

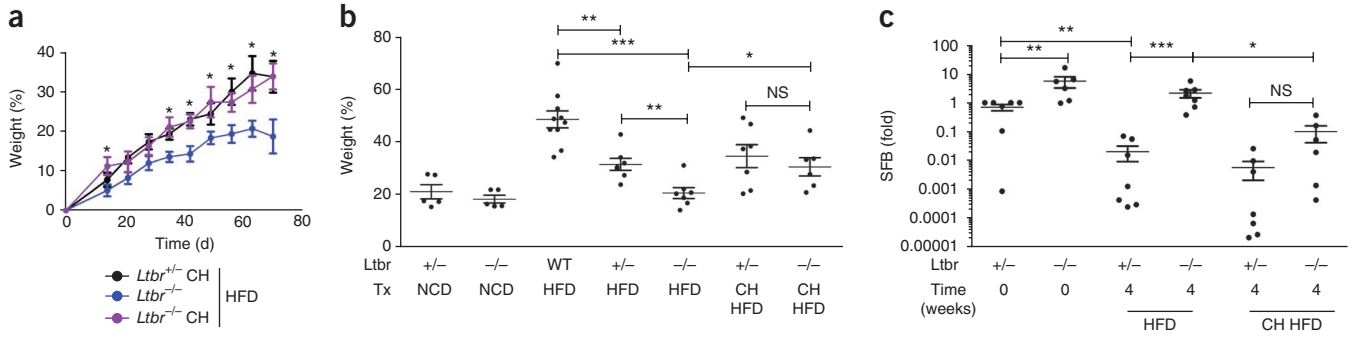

Figure 3 Environmental exposure reveals horizontal transmissibility of the obese phenotype. (**a**,**b**) For *Ltbr*$^{+/-}$ or *Ltbr*$^{-/-}$ mice that had been genotyped and weaned either separately or together (CH indicates cohoused animals) at 3 weeks of age and NCD or HFD was initiated at 9 weeks of age, weight gain during days on diet as a percentage of weight at start of diet (**a**); weight gain after 9 weeks of diet (**b**); Tx indicates combination of diet and housing conditions. (**c**) Real-time PCR for SFB plasmid CTL5-6 in stool relative to *Ltbr*$^{+/-}$ littermates stool at the start of the diet and after 4 weeks of diet according to housing conditions. $n = 5$–12 mice per group; growth curve is representative of three experiments and statistics demonstrate differences between *Ltbr*$^{-/-}$ groups; Student's *t*-test for individual points along growth curves and dot plots: $^{*}P < 0.05$, $^{**}P < 0.01$, $^{***}P < 0.001$, NS, not significant ($P > 0.05$). Error bars, s.e.m.

Because the loss of species diversity is a hallmark of the obese microbiome in humans, and because SFB were overrepresented in *Ltbr*$^{-/-}$ mice, we used SFB as a representative marker species for changes to the microbiota. The proportion of SFB was substantially reduced after heterozygous mice were placed on HFD, suggesting that HFD creates environmental changes that are unfavorable to SFB (**Fig. 3c**). These changes could be either directly through changes in nutrition or mediated by indirect mechanisms. However, *Ltbr*$^{-/-}$ mice that we housed separately from their *Ltbr*$^{+/-}$ littermates experienced very modest, if any, decreases in SFB after HFD, arguing that although both mice were subjected to a change in the nutritional source, this species-specific reduction cannot occur without intact host immunity (**Fig. 3c**). It is exciting to note that *Ltbr*$^{-/-}$ mice housed with their *Ltbr*$^{+/-}$ littermates experienced a rescued ability to reduce SFB abundance in their stool; this regained ability to clear SFB in response to HFD coincided with a rescue of weight gain in the cohoused mice (**Fig. 3c**). These data demonstrate that exposing *Ltbr*$^{-/-}$ mice to their LTβR-replete siblings not only rescued weight gain, but rescued changes in the microbiota normally induced by exposure to HFD. The transmissibility of the obese phenotype tracked with changes in the microbiota normally associated with the obese state.

LTβR regulates IL-23 and IL-22

The behavior of SFB prompted us to consider elements of the T_H17 cytokine pathway that might be regulated by LTβR, because this particular immune response relies on SFB for induction[26,28]. The abundance of transcripts encoding transforming growth factor β (TGF-β), interleukin 6 (IL-6), IL-17A and IL-17F was similar between *Ltbr*$^{+/-}$ and *Ltbr*$^{-/-}$ groups after HFD and between groups on NCD (**Fig. 4**). However, transcripts encoding IL-23p19 and IL-22, a key downstream cytokine regulated by IL-23, were reduced in *Ltbr*$^{-/-}$ mice (**Fig. 4c**,**f**). Furthermore, IL-23p19 was induced by HFD compared to NCD. Additionally, HFD resulted in a decrease in the expression of the members of the RegIII antimicrobial peptide family, which are downstream of the IL-23–IL-22 signaling pathway, but their expression after HFD was partially dependent on LTβR, as evidenced by the observation that *Ltbr*$^{-/-}$ mice had little to no expression of these antimicrobial peptides after HFD (**Fig. 4g**,**h**). The selective loss of transcripts in the IL-23 and IL-22 pathway and not the IL-17A or IL-17F pathway in LTβR-deficient mice suggested preferential involvement of this signaling axis in regulating the microbiota and DIO.

IL-23 is regulated by LTβR and necessary for DIO

To confirm the importance of the lymphotoxin signaling pathway in the production of IL-23, we cultured colons of wild-type, *Ltbr*$^{+/-}$ and *Ltbr*$^{-/-}$ mice after HFD and measured IL-23p19p40 in the supernatants by enzyme-linked immunosorbent assay (ELISA). We observed no difference in IL-23 expression between *Ltbr*$^{+/-}$ and *Ltbr*$^{-/-}$ groups on NCD; however, we observed that IL-23 was induced in *Ltbr*$^{+/-}$ mice after HFD, but this induction did not occur in *Ltbr*$^{-/-}$ mice fed HFD (**Fig. 5a**). This is an intriguing observation because LTβR has been shown to impact IL-23 production in models of *Citrobacter rodentium* infection but not in the naive state[21,22]. This finding suggests that similar to mucosal pathogenic challenge, HFD stimulus was sufficient to evoke an immune response dependent on LTβR, which resulted in expression of IL-23. To address the importance

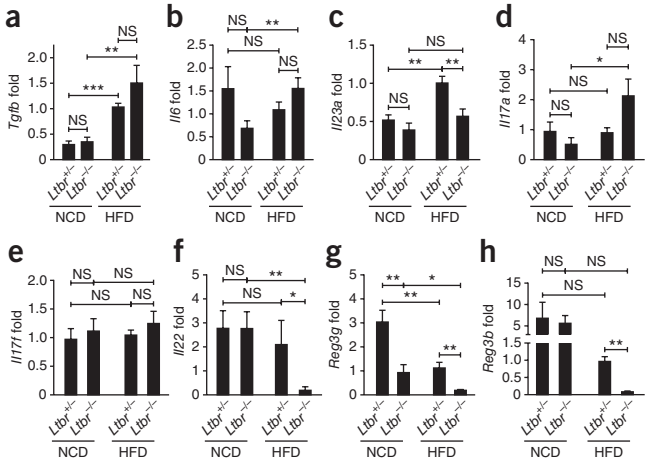

Figure 4 LTβR agonizes the innate IL-23–IL-22 axis. (**a**–**h**) Real-time PCR analysis on indicated targets on whole-colon cDNA from *Ltbr*$^{+/-}$ and *Ltbr*$^{-/-}$ mice fed HFD for 10 weeks starting at 9 weeks of age. Data are plotted relative to *Ltbr*$^{+/-}$ mice on HFD and normalized to *Hprt*. Fold indicates change in expression compared to *Ltbr*$^{+/-}$ HFD-fed mice after normalization with target gene symbol on the *y* axis; $n = 3$–9 mice per group, representative of two experiments, $^{*}P < 0.05$, $^{**}P < 0.01$, $^{***}P < 0.001$; NS, not significant ($P > 0.05$); Student's *t*-test. Error bars, s.e.m.

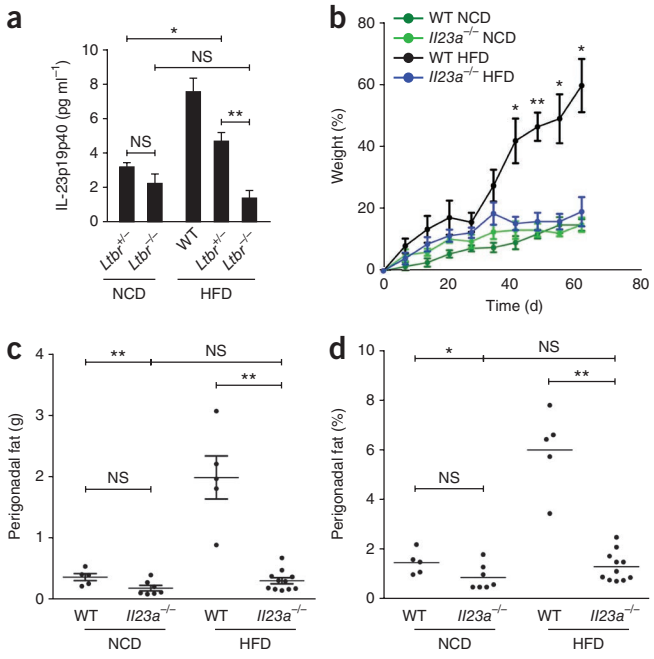

Figure 5 HFD induces LTβR-dependent IL-23, which is essential for DIO. (**a**) IL-23p19p40 production in the supernatant of colons from wild-type (WT; C57BL/6), *Ltbr*$^{+/-}$ and *Ltbr*$^{-/-}$ mice fed HFD and NCD for 10 weeks. Colons were cultured overnight and adjusted for amount of colon cultured. (**b**–**d**) For WT or *Il23a*$^{-/-}$ mice on HFD starting at 9 weeks of age for 9 weeks, weight as a percentage of starting weight (**b**); weight of perigonadal fat (**c**); and weight of fat from **c** as a percentage of body weight (**d**). $n = 5$–9 mice per group; growth curve is representative of two independent experiments and statistics demonstrate differences between HFD groups; Student's *t*-test for individual points along growth curves; one-way ANOVA with Bonferroni *post-hoc* test for dot plots: $^{*}P < 0.05$, $^{**}P < 0.01$, NS, not significant ($P > 0.05$). Error bars, s.e.m.

of IL-23 in weight gain, we challenged *Il23a*$^{-/-}$ mice with HFD; *Il23a*$^{-/-}$ mice resisted HFD induced weight gain and excess adiposity (**Fig. 5b**–**d**). Because HFD-induced IL-23 expression was dependent on LTβR, the phenotype of *Il23a*$^{-/-}$ mice is consistent with the necessity of the lymphotoxin pathway in inducing IL-23 expression for DIO.

RORγt^{+} cells are essential for weight gain after HFD

The lymphotoxin pathway is essential to enable RORγt^{+} innate lymphoid cells to produce IL-22 after acute bacterial infection[21,22]. To study whether IL-22 regulated by the lymphotoxin pathway after HFD is essential for DIO, we selected *Rorc*$^{-/-}$ mice because it has been shown that *Ltbr*$^{-/-}$ mice do not evoke IL-22 production from RORγt^{+} lymphocytes in response to acute bacterial infection[32]. We challenged *Rorc*$^{-/-}$ mice with HFD. *Rorc*$^{+/-}$ mice gained significantly more weight after HFD than their *Rorc*$^{-/-}$ littermates (**Fig. 6a**). One could argue that *Rorc*$^{-/-}$ mice may resist weight gain because of a lack of IL-23p19p40 owing to the lack of lymphoid structure in these mice, but it is important to note that IL-23p19p40 abundance was similar in colons of *Rorc*$^{+/-}$ and *Rorc*$^{-/-}$ mice (data not shown). The lymphotoxin–IL-23 axis is known to be essential in regulating IL-22 production from innate RORγt^{+} cells, and the results we obtained with *Rorc*$^{-/-}$ mice are consistent with the involvement of this lymphotoxin-mediated axis in DIO.

Consistent with our results in *Ltbr*$^{-/-}$ mice, *Rorc*$^{-/-}$ mice also sustained higher representation of SFB after HFD (**Fig. 6b**). This observation suggests that the upstream defects in immunity lead to a consistent downstream overgrowth in the microbiota. Similar to the result in *Ltbr*$^{-/-}$ mice, in the absence of RORγt^{+} cells, the perigonadal fat pad did not expand in response to HFD in *Rorc*$^{-/-}$ mice (**Fig. 6c**,**d**).

IL-22 rescues the impact of HFD on SFB and DIO

Given that HFD appeared to induce an LTβR-dependent agonism of the IL-23–IL-22 cytokine axis, we wondered whether restoring elements of this axis would rescue commensal homeostasis or weight gain in *Ltbr*$^{-/-}$ hosts. To address this question, we delivered IL-22, a construct containing both p19 and p40 subunits of IL-23 fused to an immunoglobulin region (IL-23-Ig), and IL-17A via hydrodynamic injection to *Ltbr*$^{-/-}$ adult mice at the start of a 9-week HFD. Hydrodynamic injection resulted expression of IL-22, IL-23-Ig or IL-17A detectable in the serum; IL-22 was detectable in mice treated with IL-23-Ig, although IL-17A was not (data not shown). Both IL-22 and IL-23-Ig, but not IL-17A, reduced the colonization of SFB after HFD initiation in *Ltbr*$^{-/-}$ hosts (**Fig. 7a**). Although groups treated with IL-22 or IL-23-Ig had a reduced abundance of SFB in the stool, expansion of total body size and of perigonadal fat pads occurred most extensively in *Ltbr*$^{-/-}$ mice after delivery of

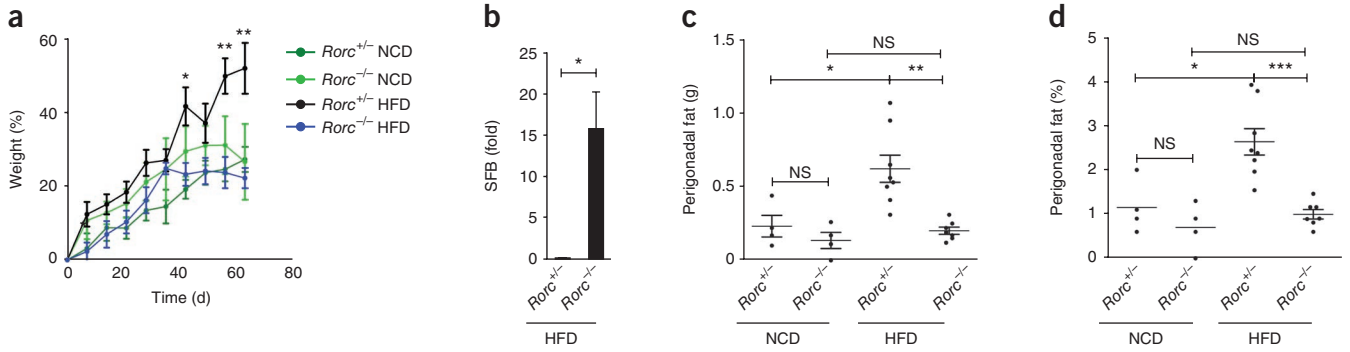

Figure 6 The transcription factor RORγt is required for weight gain and SFB homeostasis in DIO. (**a**–**d**) For *Rorc*$^{+/-}$ or *Rorc*$^{-/-}$ littermates challenged with HFD for 9 weeks starting at 5 weeks of age, weight as a percentage of starting weight (**a**); real-time PCR for SFB plasmid CTL5-6 in stool relative to *Rorc*$^{+/-}$ littermates after 4 weeks of HFD normalized to levels at the start of the diet (**b**; $n = 4$ mice in each group); weight of perigonadal fat (**c**); and weight of fat from **c** as a percentage of body weight (**d**). $n = 7$–8 mice per group; growth curve is representative of three independent experiments, and statistics demonstrate differences between HFD groups; Student's *t*-test for individual points along growth curves and SFB levels; one-way ANOVA with Bonferroni *post-hoc* test for dot plots: $^{*}P < 0.05$, $^{**}P < 0.01$, $^{***}P < 0.001$, NS, not significant ($P > 0.05$). Error bars, s.e.m.

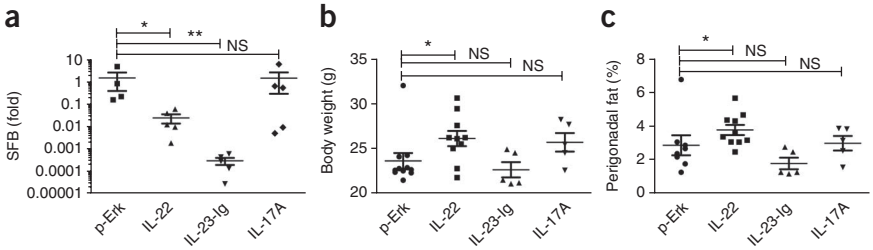

Figure 7 IL-22 restores SFB homeostasis and perigonadal fat pad expansion in *Ltbr*$^{-/-}$ mice. (**a**–**c**) For *Ltbr*$^{-/-}$ females treated with 10 μg of plasmid encoding empty vector (p-Erk IL-22, IL-23-Ig or IL-17A at the start of diet (9 weeks of age) and then subjected to a diet for 9 weeks, real-time PCR for SFB plasmid CTL5-6 normalized to day 0 of diet (**a**); total body weight (**b**) and weight of perigonadal fat pads as a percentage of body weight (**c**). $n = 5$–10 mice per group; Student's *t*-test for log-transformed data for SFB; two-tailed Mann-Whitney test for body weight and perigonadal fat because of an outlier in p-Erk group; $^{*}P < 0.05$, $^{**}P < 0.01$, NS, not significant ($P > 0.05$). Error bars, s.e.m.

IL-22 and not of IL-23-Ig or IL-17A (**Fig. 7b**,**c**). These data suggest a role for IL-22 downstream of LTβR in DIO.

DISCUSSION

Although it has been argued that diet influences the microbiota independently of host genotype[10], the possibility that innate immune responses serve as a critical pivot for species-specific responses to HFD and microbiota provides a potential link between host responses to diet, the intestinal microbiota and obesity. We observed that HFD initiates two changes in the organism: a change in the composition of the commensal microbiota and an LTβR-dependent immune response in the host. We argue that these two changes in host and microbiota are not unrelated, and in fact, changes in host immunity induced by diet actually cultivate changes in the microbial community of the distal gut. We demonstrated that the lymphotoxin–IL-23–IL-22-pathway, essential for innate immune defense against gut pathogens, is also essential for regulation of specific commensal responses to HFD.

It is thought that changes in the composition of the commensal microbiota occur as a result of altered nutritional quality of diet; in this model, the host is a static entity, not influencing the overgrowth or clearance of organisms in response to a change in diet. One study is particularly illustrative of this hypothesis and its limitations. It has been determined that unrelated mammals that consume similar diets (herbivores versus omnivores versus carnivores) maintain similar microbial communities[33]. A notable exception in the study was pandas and bears; pandas and bears are a unique group because although they are closely related, dietary composition in the group varies greatly. The microbial communities of bears, regardless of dietary habits, are similar; this exceptional group provides some evidence to support a role for the host in regulating its microbiota[34]. Additional support for the role of the host in shaping its microbial community comes from studies using reciprocal transplantation between zebrafish and mice. Mice that had been colonized with zebrafish microbiota fostered growth of the foreign bacteria, but microbes from zebrafish could only grow to abundance levels of closely related microbes that naturally grew in mice[35]. These data suggest that selective pressures in the host have some deterministic role in aspects of the microbiota, such as abundance of specific species.

HFD induced host responses would be part of the selective pressure of the gut as an ecological niche. In our model, production of antimicrobial peptides through the IL-22 (antibacterial peptide) pathway would directly antagonize the growth of some microbes, such as SFB. Species overgrowth, such as that exhibited by members of the Erysopelotrichi class, could occur in place of organisms that are eliminated by the host. In the *Ltbr*$^{-/-}$ model system, where the host lacks some elements of mucosal immunity, a change in nutrient composition was not enough to induce reductions for some bacteria, specifically SFB. When the IL-22 expression was restored in LTβR-deficient hosts, SFB was once again cleared and body size normalized. Therefore, some bacteria can become important biomarkers tracking DIO in given species.

This model presupposes the existence of an inflammatory state in the host gut induced by HFD; whereas many groups have focused on inflammation in host adipose tissue, the possibility that inflammation is not restricted to fat depots alone has had quiet support in recent years. This was initially hinted at by the finding that HFD induces expression of the transcription factor NF-κB in the colon early after the start of HFD[36]. Given the important symbiosis between the intestinal microbiota and mucosal inflammatory responses, it is logical to consider how changes in immunity influence the microbiota and, in turn, how those changes to the microbiota feedback to influence not only local immunity but systemic host health.

A major 'defect' in the microbiome of LTβR-dependent mice after HFD is that the microbial communities of *Ltbr*$^{-/-}$ mice after HFD are not less diverse. It is entirely possible that the enhanced immune response of the obese host exerts greater pressure on the microbial community of the distal gut, preventing the survival of species that could otherwise normally populate a unique niche. SFB is a useful biomarker, but the role of SFB and other species whose reduction from the gut relies on mucosal immunity for DIO remains to be determined and will benefit from gnotobiotic models and reconstitution of selective gut flora.

Even though some reports argue that genes have a large role in obesity[4,5], the consistent dysbiosis present in obese individuals suggests a strong role for environmental contribution to this disease[7]. Polymorphisms in the *Lta* locus have been linked to obesity, but the role of LTβR signaling in DIO appears to rely on changes in commensal microbiota. Moreover, the importance of this immune response on weight gain can be subverted by changes in housing. We feel that the viewpoints regarding the importance of genetics and environment are not at odds when it comes to obesity. We propose the possibility that the host response induced by HFD may actually help provide inertia for the obese state by facilitating occupation of an obese microbiome; the intestinal microbiota can thus serve as agents to transmit beneficial energy harvest to immunocompromised hosts. In the mammalian population this may be a mechanism by which mothers that are colonized with microbiota that is more efficient at energy harvest may colonize their offspring at the time of birth and before their immune systems are completely developed; from this perspective, the microbiota would facilitate more efficient use of scarce food resources.

Population-wide implications for this argument are interesting because this model suggests a potential to manipulate weight gain, either to promote or inhibit it, by regulating the microbiota through antibiotic or probiotic regimens, regulating the host through vaccination or complementary strategies using both vaccination and direct

modification of the microbiota. Even so, the precise microbes that promote such weight gain and the specific host responses that foster their growth need to be better established to create useful strategies for manipulating host-microbe interactions to influence weight gain.

METHODS

Methods and any associated references are available in the online version of the paper.

Note: Supplementary information is available in the online version of the paper.

ACKNOWLEDGMENTS

This manuscript is dedicated to the memory of Dr. Donald Liu, who provided critical efforts and support. We thank B. Becher (University of Zurich) for IL-23-Ig, C. Dong (MD Anderson Cancer Center) for IL-17, O. Wenjun (Genentech) for IL-22. V.U. was supported by the American Heart Association (AHA Predoctoral 11PRE7320015) and the US National Institutes of Health Medical Scientist Training Program grant GM007281 to the University of Chicago Pritzker School of Medicine. This research was supported by pilot grants from Digestive Diseases Research Core Center (p30 DK42086), the University of Chicago Institutional Translational Medicine (UL1 RR024999), and US National Institutes of Health grants, AI090392, DK080736 and CA134563 to Y.-X.F. T.J.K. was partially funded by the Korea Foundation for International Cooperation of Science & Technology (KICOS) grant (K20702001994-11A0500-03610).

AUTHOR CONTRIBUTIONS

V.U. participated in all experiments. T.K., A.T.V., E.P.K. contributed in the experiments shown in **Figures 1**, **4** and **5**. S.D. and S.F. contributed to the experiments shown in **Figure 2**. V.U. and V.P. performed bioinformatic analyses. L.D. contributed to the experiments shown in **Figure 7**. D.L., C.N., H.T. and E.B.C. contributed to experimental design, interpretation of results and critical assessment of the manuscript. V.U. and Y.-X.F. designed all experiments and wrote the manuscript.

COMPETING FINANCIAL INTERESTS

The authors declare no competing financial interests.

Published online at http://www.nature.com/doifinder/10.1038/ni.2403.
Reprints and permissions information is available online at http://www.nature.com/reprints/index.html.

1. Wang, Y., Beydoun, M.A., Liang, L., Caballero, B. & Kumanyika, S.K. Will all Americans become overweight or obese? Estimating the progression and cost of the US obesity epidemic. *Obesity (Silver Spring)* **16**, 2323–2330 (2008).
2. Centers for Disease Control and Prevention. Adult Obesity Facts. <http://www.cdc.gov/obesity/data/trends.html#State> (2010).
3. Flegal, K.M., Carroll, M.D., Ogden, C.L. & Curtin, L.R. Prevalence and trends in obesity among US adults, 1999–2008. *J. Am. Med. Assoc.* **303**, 235–241 (2010).
4. Stunkard, A.J., Foch, T.T. & Hrubec, Z. A twin study of human obesity. *J. Am. Med. Assoc.* **256**, 51–54 (1986).
5. Stunkard, A.J. *et al.* An adoption study of human obesity. *N. Engl. J. Med.* **314**, 193–198 (1986).
6. Turnbaugh, P.J. *et al.* An obesity-associated gut microbiome with increased capacity for energy harvest. *Nature* **444**, 1027–1031 (2006).
7. Turnbaugh, P.J. *et al.* A core gut microbiome in obese and lean twins. *Nature* **457**, 480–484 (2009).
8. Turnbaugh, P.J., Bäckhed, F., Fulton, L. & Gordon, J.I. Diet-induced obesity is linked to marked but reversible alterations in the mouse distal gut microbiome. *Cell Host Microbe* **3**, 213–223 (2008).
9. Bäckhed, F., Manchester, J.K., Semenkovich, C.F. & Gordon, J.I. Mechanisms underlying the resistance to diet-induced obesity in germ-free mice. *Proc. Natl. Acad. Sci. USA* **104**, 979–984 (2007).
10. Muegge, B.D. *et al.* Diet drives convergence in gut microbiome functions across mammalian phylogeny and within humans. *Science* **332**, 970–974 (2011).
11. Faith, J.J., McNulty, N.P., Rey, F.E. & Gordon, J.I. Predicting a human gut microbiota's response to diet in gnotobiotic mice. *Science* **333**, 101–104 (2011).
12. Eberl, G. A new vision of immunity: homeostasis of the superorganism. *Mucosal Immunol.* **3**, 450–460 (2010).
13. Henao-Mejia, J. *et al.* Inflammasome-mediated dysbiosis regulates progression of NAFLD and obesity. *Nature* **482**, 179–185 (2012).
14. Vijay-Kumar, M. *et al.* Metabolic syndrome and altered gut microbiota in mice lacking toll-like receptor 5. *Science* **328**, 228–231 (2010).
15. Norman, R.A., Bogardus, C. & Ravussin, E. Linkage between obesity and a marker near the tumor necrosis factor-alpha locus in Pima Indians. *J. Clin. Invest.* **96**, 158–162 (1995).
16. Mahajan, A. *et al.* Obesity-dependent association of the TNF/LTA locus with type 2 diabetes in North Indians. *J. Mol. Med.* **88**, 515–522 (2010).
17. Hotamisligil, G.S. Inflammation and metabolic disorders. *Nature* **444**, 860–867 (2006).
18. Wellen, K.E. & Hotamisligil, G.S. Inflammation, stress, and diabetes. *J. Clin. Invest.* **115**, 1111–1119 (2005).
19. Pamir, N., McMillen, T.S., Edgel, K.A., Kim, F. & LeBoeuf, R.C. Deficiency of lymphotoxin-alpha does not exacerbate high-fat diet-induced obesity but does enhance inflammation in mice. *Am. J. Physiol. Endocrinol. Metab.* **301**, E961–E971 (2012).
20. Fu, Y.-X. & Chaplin, D.D. Development and maturation of secondary lymphoid tissues. *Annu. Rev. Immunol.* **17**, 399–433 (1999).
21. Ota, N. *et al.* IL-22 bridges the lymphotoxin pathway with the maintenance of colonic lymphoid structures during infection with *Citrobacter rodentium*. *Nat. Immunol.* **12**, 941–948 (2011).
22. Tumanov, A.V. *et al.* Lymphotoxin controls the IL-22 protection pathway in gut innate lymphoid cells during mucosal pathogen challenge. *Cell Host Microbe* **10**, 44–53 (2011).
23. Uysal, K.T., Wiesbrock, S.M., Marino, M.W. & Hotamisligil, G.S. Protection from obesity-induced insulin resistance in mice lacking TNF-alpha function. *Nature* **389**, 610–614 (1997).
24. Turnbaugh, P.J. *et al.* The effect of diet on the human gut microbiome: a metagenomic analysis in humanized gnotobiotic mice. *Sci. Transl. Med.* **1**, 6ra14 (2009).
25. Savage, D.C. Microbial ecology of the gastrointestinal tract. *Annu. Rev. Microbiol.* **31**, 107–133 (1977).
26. Wu, H.-J. *et al.* Gut-residing segmented filamentous bacteria drive autoimmune arthritis via T helper 17 cells. *Immunity* **32**, 815–827 (2010).
27. Klaasen, H.L. *et al.* Apathogenic, intestinal, segmented, filamentous bacteria stimulate the mucosal immune system of mice. *Infect. Immun.* **61**, 303–306 (1993).
28. Ivanov, I.I. *et al.* Induction of intestinal Th17 cells by segmented filamentous bacteria. *Cell* **139**, 485–498 (2009).
29. Sczesnak, A. *et al.* The genome of Th17 cell-inducing segmented filamentous bacteria reveals extensive auxotrophy and adaptations to the intestinal environment. *Cell Host Microbe* **10**, 260–272 (2011).
30. Prakash, T. *et al.* Complete genome sequences of rat and mouse segmented filamentous bacteria, a potent inducer of Th17 cell differentiation. *Cell Host Microbe* **10**, 273–284 (2011).
31. Lathrop, S.K. *et al.* Peripheral education of the immune system by colonic commensal microbiota. *Nature* **478**, 250–254 (2011).
32. Cella, M. *et al.* A human natural killer cell subset provides an innate source of IL-22 for mucosal immunity. *Nature* **457**, 722–725 (2009).
33. Ley, R.E. *et al.* Evolution of mammals and their gut microbes. *Science* **320**, 1647–1651 (2008).
34. Vaishnava, S. *et al.* The antibacterial lectin RegIIIγ promotes the spatial segregation of microbiota and host in the intestine. *Science* **334**, 255–258 (2011).
35. Rawls, J.F., Mahowald, M.A., Ley, R.E. & Gordon, J.I. Reciprocal gut microbiota transplants from zebrafish and mice to germ-free recipients reveal host habitat selection. *Cell* **127**, 423–433 (2006).
36. Ding, S. *et al.* High-fat diet: bacteria interactions promote intestinal inflammation which precedes and correlates with obesity and insulin resistance in mouse. *PLoS ONE* **5**, e12191 (2010).

ONLINE METHODS

Mice. Wild-type (WT) C57BL/6 mice were obtained from Jackson Laboratories, Harlan Laboratories or the US National Cancer Institute. *Lta*$^{-/-}$, *Ltb*$^{-/-}$, *Ltbr*$^{-/-}$, *Il23a*$^{-/-}$ and *Rorc*$^{-/-}$ mice were bred in our vivarium at the University of Chicago. In cases of all heterozygous mice, breedings were set up where one parent was a null mouse and the other was a heterozygous mouse (usually the father). Mice were genotyped by PCR and weaned as early as 21 d and as late as 28 d after birth. Cohousing experiments were performed with three heterozygous and two homozygous null mice in a cage. Germ-free C57BL/6 mice were maintained in the gnotobiotic facility at the University of Chicago. Mice were maintained according to the standards set by the University of Chicago's Institutional Animal Care and Use Committee (protocols #71866 and #58771).

HFD and NCD challenge experiments. All specific pathogen free mice were maintained on Harlan Teklad 2918 until the start of diet, when they were either switched onto 88137 or maintained on 2918 for the duration of the experiment. Mice were weighed every 7–10 d after the start of diet. At the end of diet (63–70 d after initiation), mice were killed by CO_2 euthanasia and cervical dislocation. Mice were weighed again after killing and perigonadal fat (periuterine or epididymal fat in the case of female and male mice, respectively) was dissected and weighed.

Food consumption. Mice were started on either NCD or HFD at day 0, and food weight was measured daily. Successive weights of food were subtracted from that measured on the previous day (day n – day n + 1) and data were plotted adjusted for the number of days between food measurements, which varied between 1 and 3 d. Five mice were housed per cage.

Cecal and stool DNA extraction. Cecal samples were collected at the time of killing the mice (at the end of NCD or HFD) and frozen at −80 °C until processing. Stool samples were collected in our vivarium at 0, 4 and 9 weeks after the start of diet and frozen at −20 °C. All extraction was done using the QIAamp DNA Stool Mini Kit (Qiagen). Briefly, samples were lysed in a detergent solution and mechanically dissociated using a Mini-beadbeater (BioSpec Products) for 90 s at maximum setting. Samples were treated with InhibitEX matrix to prevent DNA damage and to inhibit PCR-disrupting agents. Subsequently, proteins were digested with proteinase K, samples were bound to a column, washed twice and eluted in the supplied buffer. Quality of DNA and concentrations were determined using Nanodrop 2000 Spectrophotometer (Thermo Scientific).

PCR amplification and 454 pyrosequencing of 16S rRNA–encoding genes. Sequencing was done on samples from two different litters of mice in two different facilities to ensure thorough understanding of microbial communities (one set of samples from one litter with V1–V2 regions prepared at the University of Chicago (primers listed at end) listed as T1; another set of samples from another litter amplified for V3–V4 regions: trial 2 listed as T2 in **Supplementary Table 2**). For T1, sequencing and analysis were done as described[37]. V1–V2 regions of 16S rDNA from stool or cecal samples were amplified with TaKaRa Ex Taq PCR mixture. The PCR program was set at 95 °C for 10 min, 30 cycles of 95 °C for 1 min, 50 °C for 1 min, 72 °C for 1.5 min, followed by 72 °C for 10 min. PCR products were purified using the AMPure Kit (Agentcourt Bioscience). The resulting product was analyzed on a 2% agarose gel and by Nanodrop. Products were then pooled at equal concentrations and sequenced on a GS Titanium 70 × 75 picotiter plate according to the manufacturer's protocols for GS FLX (Roche Applied Science) at the Roy J Carver Center at the University of Illinois at Urbana Champaign. Sequencing primers are listed in **Supplementary Table 3**. For T2, PCR primers used were specific for the V3–V5 region of 16S rRNA–encoding genes. DNA was prepared and submitted to Research and Testing Laboratories for amplification, barcoding and sequencing.

Analysis of pyrosequencing. The 16S rRNA sequence analysis was performed via MOTHUR suite of programs, version 1.17.0 (ref. 38). Low-quality sequences were trimmed, and redundant sequences were removed to create a simplified data set. Sequences were aligned to the SILVA reference database, chimeric sequences were removed, and OTU clustering was performed via average neighbor methodology. Simpson diversity index (a measure of biodiversity within a habitat) was calculated using table of OTU abundances. PCA was performed using matrix of Yue and Clayton similarity measures. To minimize complications from unclassified OTUs, phylotype-based analysis was also preformed. High-quality sequences were taxonomically annotated via the RDP classifier tool[38]. Differentially abundant features were determined via Metastats[39].

Sequence alignment. OTU alignment to the known 16S SFB rRNA encoding V1–V2 region was performed using ClustalW2 available from the European Bioinformatics Institute.

Germ-free experiments. Germ-free NCD and HFD are described in **Supplementary Table 1.** WT C57BL/6 germ-free mice were gavaged with fresh cecal contents from *Ltbr*$^{+/-}$ and *Ltbr*$^{-/-}$ donors maintained on similar diets.

Colon culture and enzyme-linked immunosorbent assay (ELISA). Proximal colon pieces weighing less than 50 mg were cut in small pieces and incubated in 0.4 ml of RPMI 1640x containing 10% FBS, amphotericin, gentamicin, penicillin and streptomycin for 48 h in tissue plates, as described[40]. IL-23p19p40 in supernatants was measured by ELISA (eBiosciences) according to the manufacturer's recommendations.

Hydrodynamic injection. Hydrodynamic injection was performed as described in ref. 22 by placing mice in a conical restraining device with an attached heating element. Ten micrograms of a plasmid vector expressing IL-23-Ig (B. Becher, University of Zurich), IL-17A (C. Dong, MD Anderson Cancer Center), IL-22 (IL-22, provided by Genentech) or empty vector (p-ERK, provided by Genentech) were injected 1 d or 2 d before the start of HFD in 1.8 ml TransIT-EE Hydrodynamic Delivery Solution (MIR 5340, Mirus Bio LLC) over a period that lasted less than 5 s (ref. 22).

Real-time PCR. RNA was extracted from colon samples frozen at −80 °C in RNALater (Life Technologies). Briefly, samples were homogenized in TRIzol Reagent (Invitrogen) and underwent phenol-chloroform extraction. The product was treated with amplification-grade DNase I (Sigma Aldrich). Product integrity was verified by running samples on 2% agarose gels. We used 2 μg of RNA to make cDNA using M-MLTV reverse transcriptase and associated buffers, dNTPs and oligo-dT primer (Promega). Samples were amplified on an ABI 7900 instrument (Applied Biosystems) using SsoFast EvaGreen Supermix (Bio-Rad Laboratories); primer concentrations were 0.5 μM in the final reaction. Correct melting temperatures for all products were verified after amplification. For all products, amplification in all samples resulted in correct melting temperatures. For IL-22 and RegIIIβ targets, amplification often resulted in multiple products and reactions with the resulted in multiple products are excluded from both groups. For IL-22, no *Ltbr*$^{-/-}$ mouse produced a product with the correct melting temperature, likely due to the low transcript abundance for this product in these mice. Amplification data for all PCRs were submitted to Real-Time PCR Miner for calculation of accurate cycle threshold (Ct) value and assessment of primer efficiency[41]. Fold relative to wild type normalized to *Hprt* was calculated using the Pfaffl method. Primers are listed in **Supplementary Table 4**.

Statistical methods. Statistical analysis for **Supplementary Table 2** was described above and is the outputted *P* value from Metastats. For all other statistical tests, raw data were input into GraphPad Prism v5 and analyzed through statistical tests available in the software.

37. Poroyko, V. *et al.* Gut microbial gene expression in mother-fed and formula-fed piglets. *PLoS ONE* **5**, e12459 (2010).
38. Schloss, P.D. *et al.* Introducing mothur: open-source, platform-independent, community-supported software for describing and comparing microbial communities. *Appl. Environ. Microbiol.* **75**, 7537–7541 (2009).
39. White, J.R., Nagarajan, N. & Pop, M. Statistical methods for detecting differentially abundant features in clinical metagenomic samples. *PLoS Comput. Biol.* **5**, e1000352 (2009).
40. Zheng, Y. *et al.* Interleukin-22 mediates early host defense against attaching and effacing bacterial pathogens. *Nat. Med.* **14**, 282–289 (2008).
41. Zhao, S. & Fernald, R.D. Comprehensive algorithm for quantitative real-time polymerase chain reaction. *J. Comput. Biol.* **12**, 1047–1064 (2005).

doi:10.1038/ni.2403